Exploring Intra-Annual Variability in pH, Dissolved Oxygen and Thermo-Haline Properties: Acoustic Implications in the Central Arabian Sea

Anu Susan Cheriyan*, P.A. Maheswaran, Harikrishnan M., Dominic Ricky Fernandez and A. Raghunadha Rao

DRDO-Naval Physical Oceanographic Laboratory, Kochi - 682 021, India *E-mail: anususancheriyan1991@gmail.com

ABSTRACT

The study aims to understand the intra-annual variability of pH, dissolved oxygen and thermo-haline properties of central Arabian Sea to discern its implications on sound absorption properties. The study was carried out utilizing one year Argo float data (WMO ID 1902458) during 2023-2024. The pH distribution exhibited a typical vertical pattern characterized by a surface maximum, a sub-surface minimum, and a gradual increase with increasing depth. The pH distribution showed a pronounced downward gradient, coinciding with a strong downward gradient in temperature and dissolved oxygen. This suggests a robust correlation between pH vs dissolved oxygen (R^2 =0.97) and pH vs temperature (R^2 =0.91) in the thermocline region. The study emphasizes the significant impact of Arabian Sea High Saline Water mass and Bay of Bengal low saline waters on pH variability. Furthermore, the findings highlight the important influence of pH fluctuations on sound absorption properties, emphasizing the need to consider these factors in oceanographic characterization.

Keywords: pH; Dissolved oxygen; Thermo-haline; Acoustics; Arabian sea

1. INTRODUCTION

The Arabian Sea (AS) located in the western part of the Northern Indian Ocean (NIO) is regarded as one of the most productive regions of the world ocean and is characterized by seasonally reversing monsoonal winds¹⁻³. This unique seasonal reversal in atmospheric forcing during summer and winter monsoon play a vital role in the variability of thermohaline structure, circulation, and biogeochemical distributions in the upper layers of water column in the AS1,3-7. In summer monsoon, the enhanced productivity in central AS is primarily attributed to the lateral advection of nutrient rich coastal waters, with minor contribution from vertical mixing⁸. Arabian Sea undergoes rapid biogeochemical changes witnessing a temperature rise, 9-11 a rise in CO₂12, and a drop in pH¹³⁻¹⁴. The sea-surface temperature and mixed layer depth in the central Arabian Sea were mainly controlled by wind forcing and incoming solar radiation⁷. The AS has one of the world's most pronounced and intense Oxygen minimum zones (OMZs)15, with previous reports indicating an expansion in AS OMZ¹⁶⁻¹⁷.

Since the beginning of the Industrial Revolution, ocean acidification has been observed and is expected to further decrease the ocean pH in the future, which has a significant impact in the operation of commercial, scientific and naval applications based on ocean acoustics¹⁸⁻¹⁹. Previous studies have reported that, for pH reduction by 0.3, from 8.1 to 7.8, has resulted in a 40 % decrease in the acoustic absorption at low frequencies (<1 KHz), leading to a considerable increase

Received: 28 February 2025, Revised: 05 May 2025

Accepted: 01 October 2025, Online published: 04 November 2025

in the ocean noise²⁰⁻²¹. The human-induced CO₂ absorbed by the ocean gets transported to the deeper layers of the water column leading to a reduction in pH of deeper waters¹¹, that has a substantial effect on the sound absorption properties used in acoustics^{18,20-21} Although few studies are available revealing the seasonal variations in pH in the surface waters of NIO²²⁻²³ and in the coastal waters of AS¹⁴, an understanding of pH variability in the sub-surface and deeper layers of Arabian Sea is still in the fundamental stage¹¹. Very recently, Shetye, et al., have documented the seasonal, temporal and spatial variations in pH and the factors influencing pH in the NIO¹¹. The vertical pH variability give an idea about vertical mixing and stratification, and also could reveal the extent of photosynthetic zone (euphotic zone), where phytoplankton conduct photosynthesis²⁴. The objectives of the study focus on assessing (1) seasonal variations of temperature, salinity, dissolved oxygen, and pH along the Argo float trajectory and the factors controlling their variability (2) the significance of pH changes in central Arabian Sea and its implications on acoustic propagation.

2. METHODOLOGY

2.1 Study Area

During summer monsoon, the strong southwesterly winds prevail and the monsoon current is strong and flows southeastward (Fig. 1(b)). During Fall Inter Monsoon, the winds are observed to be weak and a shift in the wind pattern from the southwest direction to the northeast is observed. The currents are also observed to be weak during this transition period. In winter monsoon, the northeast monsoon sets in with strong

northeasterly winds and the current flows north westward. Similar to Fall Inter Monsoon, the winds and currents during Spring Inter Monsoon are also observed to be weak.

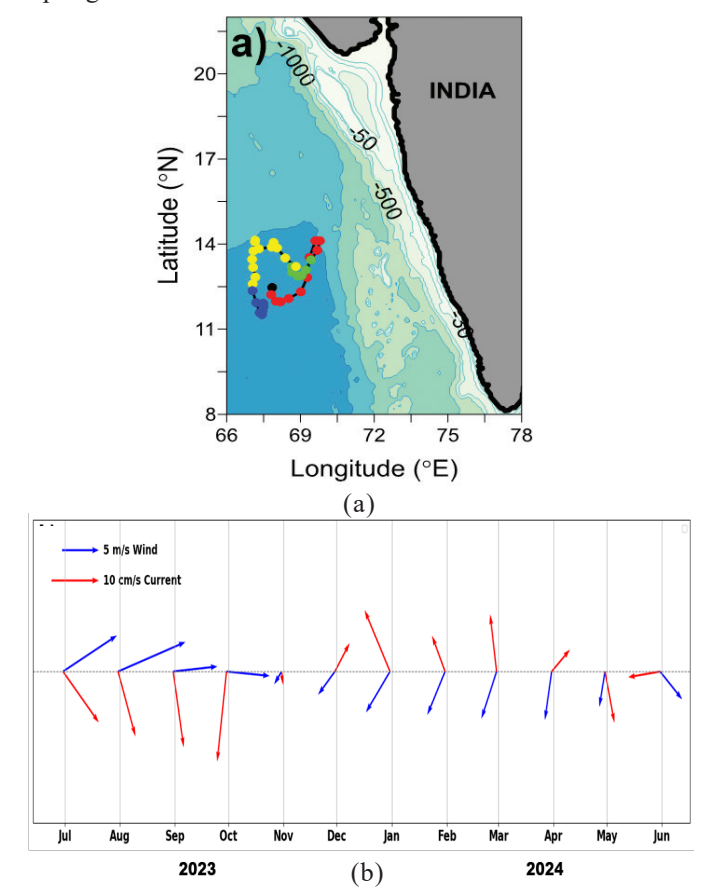


Figure 1. (a) Location map showing the trajectory of Argo float (WMO ID 1902458) during June 2023 to June 2024. Red, green, yellow and blue circles indicates the trajectories of Argo float in summer, fall, winter and spring monsoon seasons, respectively. Black circle designate the Argo float deployment location; and (b) monthly evolution of ERA 5 wind and CMEMS currents, averaged over the float location in the AS.

2.2 Data and Methods

The Argo data used in this study were obtained from the Coriolis Argo Global Data Assembly Centre, with float number WMO ID: 1902458 deployed near the south central Arabian Sea (12.5°N, 67.4°E) during June 2023. The float was equipped with a SBE41CP CTD unit to measure conductivity (salinity), temperature and an SBE 63 OPTODE 3251 dissolved oxygen sensor. In addition, the float was fitted with an SBE SEAFET 720-11597 TRANSISTOR-pH sensor for measuring the pH. The analytical precision was ~0.004 for pH. The Argo float acquire data at predetermined depths every 2 m in the upper 1000 m and every 50 m between depths of 1000 and 2000 m during their ascent and the temporal resolution was every ten days. The Argo float is still active and we specifically report data collected between 14-06-2023 and 08-06-2024. The deployment location (shown as circle) and the trajectory of the float deployed in the region are shown in Fig. 1(a).

We defined Mixed Layer Depth (MLD) as the depth at which the temperature showed 1 $^{\circ}\text{C}$ drop from its surface

value. The two water masses observed in the upper 100 m are low saline Bay of Bengal water mass (BBW; $\sigma_{\rm t} < 22~{\rm kg~m^{-3}}$, salinity 34-35 psu) and Arabian Sea High Saline water mass (ASHSW; $\sigma_{\rm t} \sim 23$ -24 kg m⁻³, salinity >36.00 psu, temperature 28-24 °C)²⁵⁻²⁷. The core of ASHSW (S_{max}) is defined as the maximum salinity value observed while the depth corresponding to this maximum salinity is designated as S_{max} D. The sound absorption was calculated using the formula put forth by Francois and Garrison [28]. We have represented the following seasons during the year: Summer Monsoon (SM; June-September), Fall Inter Monsoon (FIM; October-November), Winter Monsoon (WM; December–March), and Spring Inter Monsoon (SIM; April–May). In this study, we have focused on analysing data in the upper 500 m for dissolved oxygen and pH, and 200 m depth for other parameters.

3. RESULTS AND DISCUSSION

3.1 Observed Variability of Thermo-Haline Structure

The time-depth sections of temperature (°C) and salinity (psu) along the Argo trajectory in the upper 200 m of the water column, are exhibited in Fig. 2(a) and Fig. 2(b), respectively. The sea surface temperature (SST) in the Argo float trajectory ranged from 27.64 °C to 31.21 °C with minimum and maximum temperatures observed in the month of February and May, respectively. The average SST in SM, FIM, WM, and SIM was found to be 28.96 °C, 29.63 °C, 28.67 °C, and 30.69 °C respectively. The near-surface temperature exhibits a strong bimodal signal consistent with earlier studies,

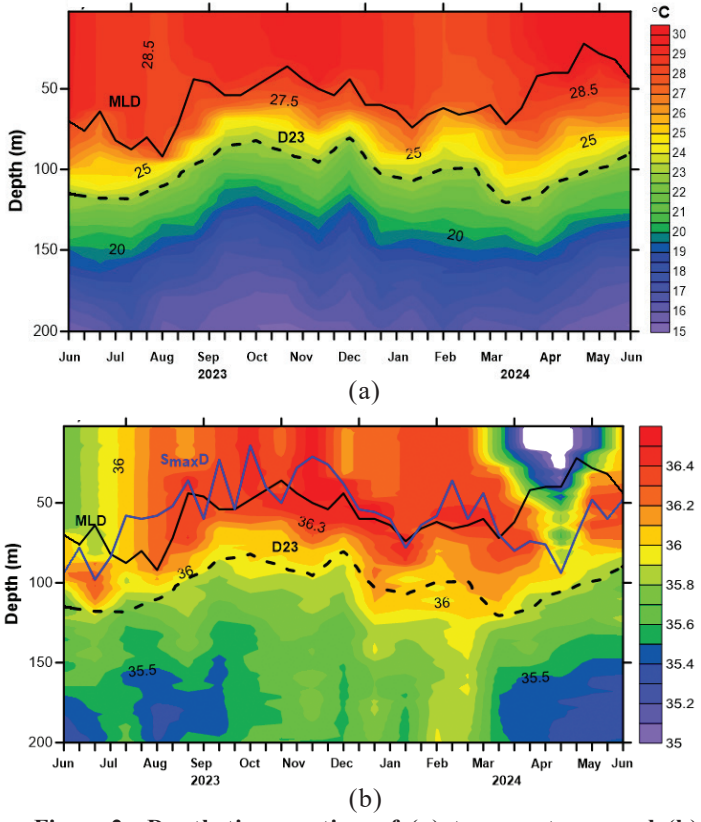


Figure 2. Depth-time section of (a) temperature; and (b) salinity along the Argo float trajectory. MLD and D23 is marked as thick black line and dashed line, respectively. S_{max} D is indicated as blue line in Fig. 2(b).

with warming observed during SIM (April-May) and FIM (October-November), and cooling observed during the SM (June-September) and WM (December-February) seasons. The SST in Arabian Sea is mostly influenced by factors such as surface heat fluxes, vertical mixing, horizontal and vertical advection^{3,5,11,29-31}. The average position of the depth of the 23 °C isotherm (D23), which is regarded as a proxy for permanent thermocline was observed around 100 m depth and it varied between 75 m to 120 m depth (Fig. 2(a)).

The MLD varied from 22 m to 92 m, with the deepest MLD observed during August and the shallowest during May. The mixed layer showed a deepening tendency after the onset of SM and it reaches its deepest MLD in August. The deepening of mixed layer can be ascribed to the strong wind-induced vertical mixing and convective overturning due to net heat loss from the surface³. From September onwards, shallowing of mixed layer is observed and the shallowest MLD is observed during SIM period. This might be due to the increasing surface net heat flux and lower wind speed conditions resulting in the warming and shallowing of mixed layer during FIM and SIM³. During WM, the MLD gets slightly deepened (74 m) compared to FIM and relatively shallower compared to SM, attributed to weak surface forcing³⁰.

The salinity data from the Argo float shows comparatively low saline waters (34.7-34.8) in the near surface layer and relatively high saline waters (>36.0) in the sub-surface layer during April-May, resulting a strong halocline in the near surface layer during SIM period (Fig. 2(b)). The increased evaporative cooling driven by dry air (low humidity) from the north leads to the convective formation of ASHSW during WM in the northern AS and it spreads southward along the constant density surface (σ_{t} ~24 kg m⁻³) [31]. It generally occurs at deeper depths (90-100 m) during April-May and relatively at shallower depths (50-60 m) during September-October in the central AS [32]. In this study, the S_{max} (core of ASHSW) ranged between 36.02 and 36.57 psu, with the minimum core value recorded at April and maximum at December (Fig. 2b). The S D extends from the surface till 100 m depth. It is evident that the core of ASHSW appears weaker in SM, while its intensity is getting stronger in WM. In the open ocean, the mixed layer salinity evolution is influenced by various processes including local fresh water flux (evaporation-precipitation), horizontal advection leading to salinity redistribution, and entrainment through the mixed layer base³. Horizontal advection in the southeastern Arabian Sea plays a significant contribution on mixed layer salinity modulation than local fresh water flux and vertical process 31,33.

In the present study, the low salinity waters observed in the near surface layer during April-May, along the float trajectory is primarily attributed to the influence of Bay of Bengal low saline water mass. During this time, the Argo float was located (~11.5°N, 67.4°E) at the southern part of its trajectory (blue circles in Fig.1), and the thermohaline indices of this low-salinity water suggest the presence of BBW. During the winter monsoon (December–February), the East India Coastal Current (EICC) bifurcates south of Sri Lanka, with one branch flowing northward as the West India Coastal Current (WICC). This current transports low-salinity Bay of Bengal

Water (BBW) into the southeastern Arabian Sea (SEAS), with the intrusion typically ceasing by February–March. However, the intruded BBW recirculates within the region and spreads southwestward, influenced by the prevailing anticyclonic eddy circulation of the Laccadive High. This low-salinity water is believed to be one of the key drivers for the formation of the Arabian Sea Warm Pool^{5,34}. Similar salinity structures in the SEAS during March–May have also been reported by Ravichandran, *et al.*³. Following the onset of SM, the clockwise gyral circulation in the AS transports relatively high saline waters from the northern AS to southern regions^{33,35}. This influx of high saline water replaces the pre-existing low salinity waters during SIM and relatively high saline waters were observed during SM, as evidently depicted in the Fig. 2(b).

3.2 Observed Variability in Dissolved Oxygen and pH

The depth-time section of dissolved oxygen (DO) and pH in the upper 500 m of the water column are displayed in Fig. 3(a) and Fig. 3(b), respectively. The vertical profile of DO shows maximum concentration of 180-200 μ M in the upper 60 m of the water column, irrespective of all the seasons. The oxycline region is observed at depths of 40-110 m. The OMZ (where the DO concentration < 22 μ M³⁶) is found in the depth range of 110-1000 m, consistent with previous studies^{3,37,38}. The oxycline region shows its shallowest (deepest) depth during October-November (June-July, March-April) associated with shoaling (deepening) of the thermocline.

At the surface, pH ranged from 7.98 to 8.04, with minimum (maximum) pH observed in June, 2023 (February, 2024). The surface waters showed higher pH in WM followed by FIM and lower pH values observed during SM and SIM period. In a study conducted in the Southeastern AS in 1962, the surface pH was observed to be 8.3²⁴, whereas the present study showed a maximum surface pH of 8.04, indicating a decline of 0.26 units over the past 62 years. The pH difference within the MLD showed only small variation, while the thermocline region exhibited a sharp gradient in pH, irrespective of all the seasons. The spatial and seasonal variations in pH is regulated by both physical and biological processes, which are in turn influenced by the seasonal reversal of monsoonal winds².

The vertical distribution of pH showed a consistent pattern in all the seasons, characterized by a surface maximum followed by a sub-surface minimum, and a gradual rise with increasing depth. The pH varied from 7.57 to 8.04, with minimum (maximum) pH observed in June, 2023 (February, 2024) at 256 m and surface layers, respectively. The higher pH values observed in the surface layers was attributed to the consumption of CO, by photosynthesis. But the pH values dropped rapidly in the sub-surface waters as a result of respiration processes releasing CO₂². The vertical pH distribution exhibited similar pattern as that of DO content, suggesting a marked relationship existing between the pH and variations in DO. The pH showed its maximum values mostly in regions where the maximum DO concentration is observed. Moreover, these high pH values at the surface is attributed to the photosynthetic removal of CO, by phytoplankton²⁴. The maximum pH is observed in the

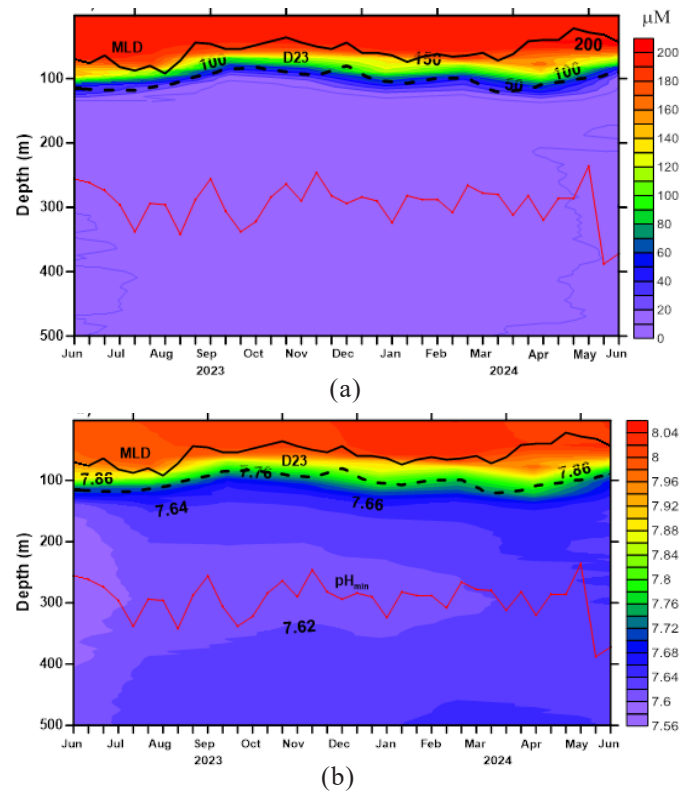


Figure 3. Depth-time section of (a) DO and (b) pH in the upper 500 m water column along the Argo float trajectory. The depth corresponding to pH minimum values (pH_{min}) in all the profiles are indicated as a thin red line in Fig. 3(a) and Fig. 3(b).

surface waters, where maximum photosynthesis takes place. In this study, the maximum pH observed zone extends from the surface till 56 m depth from June 2023 to June 2024. The maximum pH observed below the surface waters might be attributed to the occurrence of Arabian Sea high saline water mass near the surface layers. Irrespective of all the seasons, the maximum pH observed zone is found in the surface and near-surface waters.

The pH distribution exhibited a marked downward gradient, coinciding with a strong downward gradient in temperature and DO concentration. The thermocline in all the profiles marks a transition zone in pH. The lowest pH in the vertical profile of pH from June 2023 to June 2024 occurred within the depth range of 236 m to 388 m. The minimum pH value in all the profiles is observed mostly in the intense oxygen minimum zone and is clearly visible in the Fig. 3(a). The correlation analysis performed between the pH values with temperature and DO concentration in the thermocline region revealed significant relationship existing between these parameters. The scatter plots of pH vs DO (R^2 =0.97) and temperature vs pH (R^2 =0.91) designated in Fig. 4(a) and Fig. 4(b), respectively showed significant correlation.

3.3 Water Masses and pH Variability

The ASHSW typically occupies the region between the surface and the upper thermocline layer. Notably, when the core of the ASHSW is observed near the surface, there is a coincidental occurrence of pH maxima at corresponding

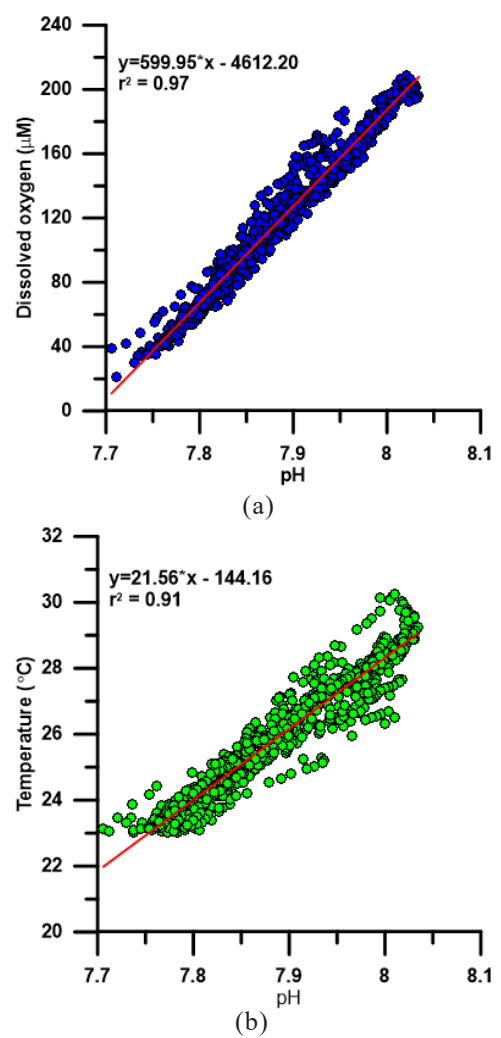


Figure 4. Scatter plots of (a) pH vs DO and (b) pH vs temperature in the thermocline region.

depths. This phenomenon is evidently observed in multiple profiles from August to October 2023 and from February to June 2024, where pH maxima occurred at depths ranging from 14 m to 56 m. Furthermore, it is intriguing to observe that the pH exhibited a weak gradient at depths corresponding to the ASHSW. This weak pH gradient is attributed to the ASHSW, which typically forms in the northern Arabian Sea due to intense evaporation and associated convective mixing. The influence of low saline BBW in the study region during April-May leads to a decrease in pH values in the surface waters. This might be due to the elevated acidification rates reported in the coastal Bay of Bengal resulting from anthropogenic input of pollutants to the atmosphere and subsequent deposition instigating significant decline in pH³⁹.

3.4 Impact of pH Variations on Sound Absorption Properties

Figure 5 illustrates the intricate relationship between sound absorption, frequency, and pH in the South Central AS. Utilizing the Francois and Garrison Method, sound absorption values (in dB) were calculated across a frequency spectrum ranging from 500 Hz to 10 kHz, corresponding to pH values ranging from 8.04 to 7.6 at depths ranging from the surface

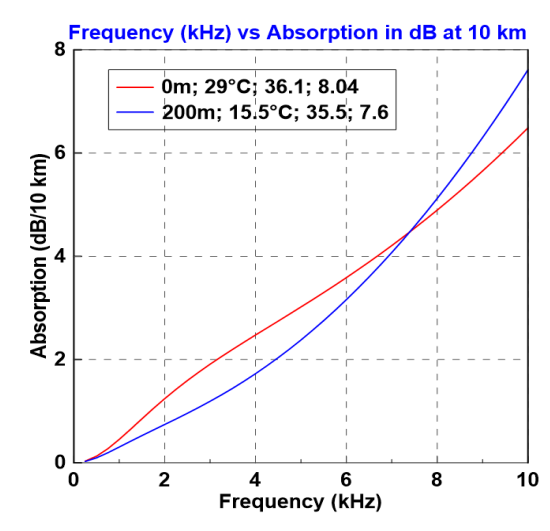


Figure 5. Illustration of the non-linear change in sound absorption at 10 km range (in dB) across a frequency range from 500 Hz to 10 kHz, showcasing the impact of pH variation from 8.04 to 7.6 from surface to 200 m depth.

to 200 m²⁸. The calculations were based on mean temperature and salinity values of 29 °C and 36.1 for the surface, and 15.5 °C and 35.5 for 200 m depth. Notably, a significant decrease in absorption was observed for pH values at 200 m depth, particularly for frequencies up to 7.5 kHz. Conversely, an increase in absorption was noted for higher frequencies (>8 kHz). Specifically, the reduction in absorption values for frequencies of 4 kHz amounted to \sim 30 %, while there was a corresponding increase of \sim 20 % for frequencies of 10 kHz, thus emphasizing the complex relationship between pH and frequency-dependent sound characteristics.

5. CONCLUSIONS

The study investigates the seasonal variations in temperature, salinity, dissolved oxygen and pH in the upper 200 m along the Argo float trajectory in Central AS from June 2023 to June 2024. SST ranged from 27.64 °C to 31.21 °C, with maximum (minimum) temperatures observed in May (February). The MLD exhibited a deepening tendency after the onset of SM, reaching a maximum depth of 92 m in August, attributed to wind-induced vertical mixing and convective overturning. Conversely, shallowing of mixed layer was observed during FIM and SIM, reaching its minimum MLD during May, likely due to increased surface net heat flux and lower wind speeds. The ASHSW extended up to 150 m depth, with the core salinity (S_{max}) ranging from 36.04 to 36.57 psu, exhibiting seasonal variations. The core of ASHSW appears weaker in SM, while its intensity is getting stronger in WM. A strong halocline was observed in the near surface layer during SIM period due to the intrusion of low saline BBW into the study region. The pH in the surface layers ranged from 7.98 to 8.04, with minimum (maximum) pH observed in June, 2023 (February, 2024). The higher pH values observed in all profiles are associated with higher temperature and greater dissolved oxygen content. The minimum pH value in all the profiles is observed mostly in the intense oxygen minimum zone below the thermocline region. The scatter plot analysis revealed

significant correlation existing between pH vs temperature $(R^2=0.91)$ and pH vs DO $(R^2=0.97)$ in thermocline region. The study also highlights the role of ASHSW and BBW in regulating pH variability. These findings underscore the substantial impact of pH variations on sound absorption properties in the Central Arabian Sea, highlighting the complex interplay between oceanic acidity, sound propagation, and frequency-dependent absorption characteristics.

REFERENCES

- 1. Madhupratap M, Kumar SP, Bhattathiri PM, Kumar MD, Raghukumar S, Nair KK, Ramaiah N. Mechanism of the biological response to winter cooling in the northeastern Arabian Sea. Nature. 1996 Dec 12;384(6609):549-52.
- Omer W. Ocean acidification in the Arabian Sea and the Red Sea. University of Bergen, Norway, 2010. (Master's thesis).
- 3. Ravichandran M, Girishkumar MS, Riser S. Observed variability of chlorophyll-a using Argo profiling floats in the southeastern Arabian Sea. Deep Sea Research Part I: Oceanographic Research Papers. 2012 Jul 1;65:15-25.
- Kumar SP, Madhupratap M, Kumar MD, Gauns M, Muraleedharan PM, Sarma VV, De Souza SN. Physical control of primary productivity on a seasonal scale in central and eastern Arabian Sea. Journal of Earth System Science. 2000 Dec;109(4):433-41. doi: 10.1007/BF02708331.
- Rao RR, Sivakumar R. Seasonal variability of nearsurface thermal structure and heat budget of the mixed layer of the tropical Indian Ocean from a new global ocean temperature climatology. Journal of Geophysical Research: Oceans. 2000 Jan 15;105(C1):995-1015. doi:10.1029/1999JC900220.
- Prasanna Kumar S, Narvekar J, Kumar A, Shaji C, Anand P, Sabu P, Rijomon G, Josia J, Jayaraj KA, Radhika A, Nair KK. Intrusion of the Bay of Bengal water into the Arabian Sea during winter monsoon and associated chemical and biological response. Geophysical Research Letters. 2004 Aug;31(15). doi:10.1029/2004GL020247.
- Kumar SP, Narvekar J. Seasonal variability of the mixed layer in the central Arabian Sea and its implication on nutrients and primary productivity. Deep Sea Research Part II: Topical Studies in Oceanography. 2005 Jul 1;52(14-15):1848-61.
- 8. Kumar SP, Madhupratap M, Kumar MD, Muraleedharan PM, De Souza SN, Gauns M, Sarma VV. High biological productivity in the central Arabian Sea during the summer monsoon driven by Ekman pumping and lateral advection. Current Science. 2001 Dec 25:1633-8.
- 9. Roxy MK, Ritika K, Terray P, Masson S. The curious case of Indian Ocean warming. Journal of Climate. 2014 Nov 15;27(22):8501-9.
- Sun C, Li J, Kucharski F, Kang IS, Jin FF, Wang K, Wang C, Ding R, Xie F. Recent acceleration of Arabian Sea warming induced by the Atlantic-western Pacific transbasin multidecadal variability. Geophysical Research Letters. 2019 Feb 16;46(3):1662-71.

- 11. Shetye S, Kurian S, Shenoy D, Gauns M, Pratihary A, Shirodkar G, Naik H, Fernandes M, Vidya P, Nandakumar K, Shaikh A. Contrasting patterns in pH variability in the Arabian Sea and Bay of Bengal. Environmental Science and Pollution Research. 2024 Feb;31(10):15271-88.
- 12. Kanuri VV, Gijjapu DR, Munnooru K, Sura A, Patra S, Vinjamuri RR, Karri R. Scales and drivers of seasonal pCO2 dynamics and net ecosystem exchange along the coastal waters of southeastern Arabian Sea. Marine pollution bulletin. 2017 Aug 15;121(1-2):372-80.
- 13. Piontkovski SA, Queste BY. Decadal changes of the Western Arabian sea ecosystem. International Aquatic Research. 2016 Mar;8(1):49-64.
- 14. Shetye SS, Naik H, Kurian S, Shenoy D, Kuniyil N, Fernandes M, Hussain A. pH variability off Goa (eastern Arabian Sea) and the response of sea urchin to ocean acidification scenarios. Marine Ecology. 2020 Oct;41(5):e12614.
- 15. Naqvi SW, Naik H, Pratihary A, D'souza W, Narvekar PV, Jayakumar DA, Devol AH, Yoshinari T, Saino T. Coastal versus open-ocean denitrification in the Arabian Sea. Biogeosciences. 2006 Dec 14;3(4):621-33.
- Lachkar Z, Lévy M, Smith S. Intensification and deepening of the Arabian Sea oxygen minimum zone in response to increase in Indian monsoon wind intensity. Biogeosciences. 2018 Jan 10;15(1):159-86.
- 17. Lachkar Z, Lévy M, Smith KS. Strong intensification of the Arabian Sea oxygen minimum zone in response to Arabian Gulf warming. Geophysical Research Letters. 2019 May 28;46(10):5420-9.
- 18. Caldeira K, Wickett ME. Anthropogenic carbon and ocean pH. Nature. 2003 Sep 25;425(6956):365.
- Ilyina T, Zeebe RE, Brewer PG. Future ocean increasingly transparent to low-frequency sound owing to carbon dioxide emissions. Nature Geoscience. 2010 Jan;3(1):18-22
- Hester KC, Peltzer ET, Kirkwood WJ, Brewer PG. Unanticipated consequences of ocean acidification: A noisier ocean at lower pH. Geophysical research letters. 2008 Oct;35(19).
- 21. Reeder DB, Chiu CS. Ocean acidification and its impact on ocean noise: Phenomenology and analysis. J. Acoust. Soc. Am., 2010, 128(3), EL137-EL143.
- Sreeush MG, Rajendran S, Valsala V, Pentakota S, Prasad KV, Murtugudde R. Variability, trend and controlling factors of Ocean acidification over Western Arabian Sea upwelling region. Marine Chemistry. 2019 Feb 20;209:14-24.
- 23. Chakraborty K, Valsala V, Bhattacharya T, Ghosh J. Seasonal cycle of surface ocean pCO2 and pH in the northern Indian Ocean and their controlling factors. Progress in Oceanography. 2021 Nov 1;198:102683.
- Rao DS, Madhavan N. On some ph measurements in the Arabian Sea along the west coast of India. Journal of the Marine Biological Association of India. 1964;6(2):217-21.
- Kumar SP, Prasad TG. Formation and spreading of Arabian Sea high-salinity water mass. Journal of Geophysical

- Research: Oceans. 1999 Jan 15;104(C1):1455-64.
- Shenoi SS, Shankar D, Michael GS, Kurian J, Varma KK, Kumar MR, Almeida AM, Unnikrishnan AS, Fernandes W, Barreto N, Gnanaseelan C. Hydrography and water masses in the southeastern Arabian Sea during March

 –June 2003. Journal of earth system science. 2005 Oct;114(5):475-91.
- 27. Kumar PVH, Joshi M, K.V. Sanilkumar, Rao AD, Anand P, Kumar KA, et al. Growth and decay of the Arabian Sea mini warm pool during May 2000: Observations and simulations. Deep Sea Research Part I Oceanographic Research Papers. 2008 Dec 26;56(4):528–40. doi:10.1016/j.dsr.2008.12.004.
- 28. Francois RE, Garrison GR. Sound absorption based on ocean measurements. Part II: Boric acid contribution and equation for total absorption. The Journal of the Acoustical Society of America. 1982 Dec 1;72(6):1879-90.
- Shenoi SSC, Shankar D, Shetye SR. Differences in heat budgets of the near-surface Arabian Sea and Bay of Bengal: implications for the summer monsoon. J. Geophys. Res., 2002, 107:C6.
- Prasad TG. A comparison of mixed-layer dynamics between the Arabian Sea and Bay of Bengal: Onedimensional model results. Journal of Geophysical Research: Oceans. 2004 Mar;109(C3). doi:10.1029/2003JC002000.
- 31. Prasad TG. A numerical study of the seasonal variability of Arabian Sea high-salinity water. Journal of Geophysical Research. 2002;107(C11). doi:10.1029/2001JC001139.
- 32. Joseph S, Freeland HJ. Salinity variability in the Arabian Sea. Geophys Res Lett. 2005;32:L09607. doi:10.1029/2005GL022972.
- 33. Rao RR. Seasonal variability of sea surface salinity and salt budget of the mixed layer of the north Indian Ocean. Journal of Geophysical Research. 2003;108(C1). doi:10.1029/2001JC000907.
- Rao RR, Jitendra V, GirishKumar MS, Ravichandran M, Ramakrishna SS. Interannual variability of the Arabian Sea Warm Pool: observations and governing mechanisms. Climate Dynamics. 2015 Apr;44(7):2119-36.
- 35. Jensen TG. Cross-equatorial pathways of salt and tracers from the northern Indian Ocean: Modelling results. Deep Sea Research Part II: Topical Studies in Oceanography. 2003 Jul;50(12-13):2111–27. doi:10.1016/S0967-0645(03)00048-1.
- Gibson RN, Atkinson RJ. Oxygen minimum zone benthos: adaptation and community response to hypoxia. Oceanogr. Marine Biol. Annu. Rev. 2003 Jul 31;41:1-45.
- 37. Rochford DJ. Source regions of oxygen maxima in intermediate depths of the Arabian Sea. Marine and Freshwater Research. 1966;17(1):1-30.
- 38. Naqvi W.A. Some aspects of the oxygen-deficient conditions and denitrification in the Arabian Sea. J. Mar. Res., 1987, 45, 1049–1072.
- 39. Sarma VV, Krishna MS, Srinivas TN, Kumari VR, Yadav K, Kumar MD. Elevated acidification rates due

to deposition of atmospheric pollutants in the coastal Bay of Bengal. Geophysical Research Letters. 2021 Aug;48(16):e2021GL095159.

ACKNOWLEDGEMENT

We would like to thank the Director, DRDO-NPOL for the encouragement, support and facilities provided. The first author gratefully acknowledges DRDO Research Associateship (No.NPOL/A/EST/127/SRF/JRF) through Naval Physical Oceanographic Laboratory for the funding support. We thank Dr. Eldhose Cheriyan and Dr. Navaneeth K.N for help in preparing the plots and their useful suggestions and discussions. The Argo float data is taken from https://www.euro-argo.eu/Argo-Data-access. ERA 5 wind data are downloaded from http://apdrc.soest.hawaii.edu/las/v6/dataset?catitem=16376. CMEMS current data were downloaded fromhttps://data.marine.copernicus.eu/product/GLOBAL_ANALYSIS FORECAST.

CONTRIBUTORS

Dr Anu Susan Cheriyan obtained her PhD in Marine Chemistry from Cochin University of Science and Technology, Kochi. She is presently engaged as Research Associate at DRDO-NPOL, Kochi. Her research areas include: Ocean biogeochemistry and environmental impact assessment.

In the present study, she has carried out the data curation, performed statistical analysis, preparation of figures and writing the manuscript with input from all authors.

Dr P.A. Maheswaran obtained his PhD in physical oceanography and working as a Scientist F at DRDO-NPOL. His research interest include: Mixed layer dynamics, sonar oceanography, conceptualized and designed the study, formulated objectives, directed data analysis.

In the current study she contributed to interpretation and discussion.

Dr Harikrishnan M. obtained his PhD in Physical Oceanography and working as a Scientist G at DRDO–NPOL. His research interest include: Upper ocean dynamics, observational oceanography. In the current study he provided expertise in upper ocean processes, guided observational strategies, and supported the study's execution.

Mr Dominic Ricky Fernandezh obtained his MSc in Oceanography and working as a Scientist F at DRDO–NPOL. His research interest include: Ocean data processing.

In the current study he did numerical model validation, analyzed data, prepared plots, and assisted in manuscript editing and review.

Dr A. Raghunadha Rao obtained his PhD in Physical Oceanography and working as a Scientist G at DRDO-NPOL. His research interest include: Tropical ocean processes, air—sea interaction. In the current study he overall supervised the manuscript, did editing and review the manuscript.